MULTIWAVELENGTH LASER PROPAGATION STUDY -- II

Quarterly Progress Report No. 2

J. Richard Kerr

Oregon Graduate Center
for Study and Research
Portland, Oregon

January, 1970

Sponsored by

Advanced Research Projects Agency
ARPA Order No. 306

ACKNOWLEDGEMENT

This research was supported by the Advanced Research Projects Agency of the Department of Defense, and was monitored by the Office of Naval Research under Contract N00014-68-0461-0001.

CONTENTS

TABLES

SUMMARY

In conducting multiwavelength scintillation experiments over a one mile path, it was found that a finite-sized transmitter aperture does not represent a true spherical-wave source, regardless of the beam divergence used. This observation has important implications for the interpretation of other data on the "saturation" of scintillations, and in the present experiments has lead to the redesign of the transmitter to achieve a virtual point source. This has been completed, including a provision for independently increasing the aperture at each wavelength up to two inches in diameter, for later transmitter-aperture-dependence measurements.

A highly-developed thermal probe system for the detailed study of turbulence structure was made completely operational, and a portable laser system was fabricated for independent "optical turbulence strength" measurements. All subsystems of the experimental facility are operating without problems, and no further modifications are contemplated.

In order to put the problem of atmospheric scintillations in current perspective and to guide the comprehensive experiments, a discussion of recent experimental and theoretical issues is given. It is felt that the understanding of the turbulence scattering problem has progressed to the point where the correct questions may be posed and definitively investigated through these experiments.

I. INTRODUCTION

The fundamental goals and experimental approach for this program were reviewed in the preceding Quarterly Progress Report. During the subsequent period, the influence of the transmitter aperture on experimental results was found to be substantial, a result which has important implications regarding the interpretation of "saturation" of scintillations as observed by other investigators. The multiwavelength transmitter was modified in order to achieve a definite equivalent to a point source, and consequently, true spherical-wave saturation measurements may now be conducted for the first time. In addition, separately and continuously variable apertures are available up to two inches in diameter at each transmitter wavelength.

A highly-developed thermal probe system for the detailed study of turbulence structure was made completely operational, and a portable laser system was fabricated for short-range, "optical turbulence strength" measurements. All subsystems of the experimental facility are operating without problems, and no further modifications are contemplated.

Highly inclement weather conditions, including consistent fog or rain, precluded the gathering of comprehensive data subsequent to the completion of final system additions described above. The remainder of the program will be devoted entirely to the use of the system to obtain data relevant to the atmospheric model, the wavelength and parameter-dependence of the onset of multiple scattering or saturation, and the influence of a finite transmitter aperture under saturated and non-saturated conditions. As discussed in Section III, it is felt that the understanding of the turbulence scattering problem has progressed to the point where the correct questions may be posed and definitively investigated through these experiments.

The final subsystem developments and typical experimental results will be described in Section II. In Section III, various aspects of other

experimental and theoretical efforts will be discussed, in order to put the overall problem in current perspective. Future plans on this program will be restated in Section IV.

II. PROGRESS DURING THIS QUARTER

A. TRANSMITTER APERTURE DEPENDENCE

Contrary to a statement in the preceding report, it was found experimentally that the effects of a finite, diverging transmitter aperture are highly important, and that the realization of a virtual point source requires careful design. The use of a point source is highly desirable when the fundamental aspects of saturation are being explored, i.e. free of aperture influences, and the implications are important in interpreting the saturation data reported by other investigators. This will be further discussed in Section III.

The fact that divergent but nonzero transmitter apertures fail to yield point-source results was suggested to the present investigator by Carlson[1]. The influence of the transmitter aperture and focusing on scintillation results has been rigorously analyzed within the single-scattering realm by Ishimaru and Carlson,[2,3,4] and semi-quantitatively by Fried.[5] Unfortunately, the work of Ishimaru and Carlson has not been reduced to numerical curves over a significant range of parameter values. In particular, for a collimated beam it has been shown[4] that as the aperture size is reduced from a very large Fresnel number (N) to a very small N, the variance of log-amplitude scintillations should decrease from the plane-wave value through a minimum (at $N \approx 1$) and then increase to the final value for a spherical wave or point source[6] (Figure 1). For a focused beam, the minimum is even sharper,[5] representing "transmitter aperture averaging." For the transmitter as described in the preceding Quarterly Report, the value of N at the shortest (4880 Å) wavelength was on the order of unity, so that a change to a point source would be expected to result in an increase in scintillation.

However, as shown in Figure 1, the opposite effect occurred in our experiments. Starting with a one-inch diameter beam which was diverged to a 1 milliradian angle, successively-smaller aperture stops were placed over the output window. The results are summarized in Table I, and indicate a significant decrease in scintillations for a point source as opposed to a source with $N \approx 1$. The change was less pronounced under high-scintillation conditions, but in either case is readily repeated and easily discernible by eye.

Aperture Size	Log-Amplitude Variance	
1"	0.13	0.45
1/4"	0.05	0.32
1/8"	0.04	0.25

Table I. Variance vs. Transmitter Aperture (4880 Å) (One Mile Path)

The theoretical curve in Figure 1 fails to predict the experimental results because the transmitter was highly divergent. The parameter a_2, which indicates defocusing, was much larger than explicitly covered in the analysis of Ref. 3, so that actual numerical predictions for this situation have not yet been given.

The effect observed here has important implications in relation to other commonly-quoted measurements of saturation, as discussed further in Section III. For the present case, it became apparent that a diverging beam is insufficient for the application of point-source theory.

In order to realize a multiwavelength transmitter with independent aperture-adjustment capabilities at each wavelength, including the achievement of a virtual point source, it was necessary to eliminate the constraint represented by the single 9 kHz chopping wheel located at the input

focus of the transmitting telescope. As reported previously, we have been able to eliminate synchronous detection while retaining our dynamic range, and hence we are permitted to use separate, smaller chopping units at the foci of beam-forming lenses at the output of each of the three lasers. Through the use of electronic etching techniques and ultra-precise machining, choppers were developed which are free of residual line-locked vibration and wobble, hence eliminating small instrumental spectrum and covariance components in the received scintillations.[7]

The point source configuration of the transmitter was designed by first choosing a diffraction-limited, collimated divergence of two milliradians at 4880 Å and 10.6 microns, which represents sufficient spread for a "spherical wave"[8] while preserving a high enough power density on the small receiver apertures to maintain the required dynamic range. Refracting optics were then utilized to match the two respective lasers, through the combining mirrors, to the off-axis parabolic output telescope such that beam waists of the proper size appear at the output window.[9] Furthermore, by sliding certain lenses beyond the chopping wheel, the output beam sizes at these two wavelengths may be independently varied up to two inches in diameter (unobstructed). In the point-source condition, the inverse Fresnel number (a_1 L in Refs. 2-4) is 4,200 at 4880 Å and 194 at 10.6 microns, resulting in definite point-source characteristics.*

At the intermediate wavelength of 1.15 microns, the laser power, mode limitations, and dynamic range conditions are such that the collimated, two-inch-diameter beam cannot be decreased in size, since greater divergence would result. However, since the laser radiation has substantial transverse mode structure, the effective aperture may be expected to be significantly smaller than the physical beam size.

---

*Further aperturing at 10.6 microns showed no effect on measured variances.

B. MEASUREMENTS WITH POINT-SOURCE TRANSMITTER

An example of simultaneous, multiwavelength data gathered with the point-source configuration at 4880 Å and 10.6 microns is given in Table II. The data were taken in the early afternoon, with hazy sky and light wind conditions. The probability distributions at each wavelength were accurately log normal.

	4880 Å	1.15 μ	10.6 μ
Log-amplitude variance from computer	0.36	0.26	0.011
Log-amplitude variance from probability slope	0.38	0.24	0.012
Amplitude correlation length at receiver (cm)	2.38	-	11.0
Bandwidth of scintillations (Hz)	35	22	-

Table II. Scintillation Data with New Transmitter Configuration (One Mile Path)

The ratio of variance at 10.6 microns vs. 4880 Å is 33, which may be compared to the theoretical ($k^{7/6}$) value of 36. However, the variance at 1.15 microns is 70% higher than its theoretical value, relative to 4880 Å, thus indicating that transmitter aperture effects are important at that wavelength; this is unavoidable, as discussed above.

The amplitude correlation length of 2.38 cm at 4880 Å may be compared with the theoretical $(\lambda L)^{1/2}$ value of 2.80 cm, while the experimental and theoretical values at 10.6 microns are 11.0 and 12.9 respectively. Due to a temporary malfunction, no value was obtained at 1.15 microns.

The scintillation bandwidths were quite small, due to the light wind conditions. The ratio of bandwidths at 4880 Å and 1.15 microns was 1.59, compared to a theoretical $(\lambda)^{1/2}$ ratio of 1.54, thus indicating that the covariance may not be seriously affected by the finite transmitter at 1.15 microns. The bandwidth at 10.6 microns was too low for measurement under such light wind conditions; this is not the usual case.

It is not clear from the above data whether the variances were saturated during this run. This is discussed further in Section III. As soon as weather permits, comprehensive data will be taken to establish the true point-source wavelength-dependence of saturated variance and covariance, as discussed in the previous report and Section III. In particular, the previously mentioned possibility that saturated variances follow the $k^{7/6}$ law will be proven or disproven.

It should be noted that under conditions of substantial rain, which has prevailed recently, the scintillations are observed to be much faster, with spectra at each wavelength up to 500 Hz, and very small amplitude correlation lengths. The effects of turbulence scattering cannot be studied under such conditions.

C. OPTICAL TURBULENCE STRENGTH MEASUREMENT SYSTEM

It was decided that there would be substantial value in incorporating a provision for measuring the "optical strength of turbulence" using a short-range laser link, as described in Ref. 10. Since the scintillation from a laser at e.g. 500 feet is small, the single-scattering (Rytov) theory applies without questions of saturation, and an independent determination of the refractive index structure constant (C_n) is obtained.[11]

In order to achieve this, we have modified 1-milliwatt He-Ne laser (6328 Å) to incorporate electronic chopping, and have mounted the unit on a tripod and cart with portable filament and high-voltage bettery supplies. The laser is bore-sighted with a rifle scope, and may be steered-in rapidly. The beam is shape to comprise a true point source. The receiver is equipped with an S-20 photomultiplier and 10-angstrom background filter for this signal, and the variance is rapidly measured using the regular system computer. This system is complementary to the thermal C_n instrument which will now be described.

D. THERMAL MICROPROBE

During the past quarter, a highly sensitive and stable thermal microprobe for the direct measurement of the refractive index (temperature) structure constant became operational. The instrument is a refinement of a concept previously described[12-14], and incorporates feedback-stabilization against drift and a low-noise subcarrier bridge technique. The electronics and operational characteristics are discussed in detail in Appendix A, along with calibration and data-reduction procedures. The capabilities of the instrumentation will be reviewed in the present section.

The instrument, shown in Figure 2, consists of two fine wire thermal probes with a variable separation; and portable, tripod-mounted electronics which process the instantaneous, fluctuating difference in the temperatures at the probes. The mean-square of this difference is presented on a built-in meter with a long averaging time constant. Appropriate gain settings are chosen with the aid of a fast-response saturation indicator. The dynamic range of the instrument covers C_n^2 values from 1.2×10^{-11} $m^{-2/3}$ to 6×10^{-17} $m^{-2/3}$, which more than brackets real values at the ground.

An output which is proportional to the instantaneous temperature fluctuations is provided which, through the use of a long cable, permits

the spectral and probability distribution analysis of the fluctuations. These analyses utilize the scintillation-computer electronics.

An example of temperature fluctuations is shown in Figure 3. The vertical scale calibration is 0.07° C per division and the sweep speed is 500 msec/cm. On this particular day, the thermal probe indicated a C_n^2 of 2.9×10^{-15} $m^{-2/3}$, and the wind was very light. On highly turbulent days, fluctuations of more than 10 times those shown in Figure 3 may be observed.

The probability distribution of fluctuations such as those shown in Figure 3 is expected to be gaussian. It must be noted, however, that recent experiments[10] have indicated the presence of anomalous spikes which may indicate plumes or other irregularities near the ground. We have not seen such irregularities, nor the attendant "tail" on the probability distribution, but weather conditions have permitted little data-taking since the system became operational. Under stable conditions, the probability tail may be expanded and examined in detail.

Under these conditions of light wind, it is not unusual for the atmospheric statistics to be highly nonstationary over time periods necessary for properly-averaged measurements. For example, immediately subsequent to the meter readout of $C_n^2 = 2.9 \times 10^{-15} m^{-2/3}$ above, probability-slope determinations of $\langle(\Delta T)^2\rangle$ showed values which changed abruptly and ranged from 4.5×10^{-15} to 7.8×10^{-16}. An example is shown in Figure 4, in which C_n^2 changed suddenly during a probability run. The points are transcribed to probability paper from the continuous, smoothed experimental plot obtained on an XY recorder.

The spectrum of the fluctuations of Figure 3 is shown in Figure 5. For an average wind velocity of 0.5 m/sec, the observed cutoff frequency of 60 Hz implies an inner scale of turbulence[11] of 0.75 cm. This rather large value indicates the low energy at such low wind levels, and can

appreciably affect the scintillation statistics, as discussed further in Section III. As discussed in Appendix A, it is possible to investigate the theoretical $f^{-5/6}$ dependence of the rms ΔT spectrum using the present equipment and a slightly modified technique.

Within the inertial subrange, the Kolmogorov theory[11] predicts that the mean-square temperature difference between the two thermal probes will vary as the 2/3 power of their separation. This will be investigated experimentally with the above system.

A preliminary measurement of the height-dependence of C_n^2 near the ground showed the value to be 40% lower at 81 inches than at 45 inches; hence, the determination should be made at the actual beam height. In addition, under stable conditions the uniformity along the path may be checked, utilizing the portability of the instrument. However, due to the coincident path nature of these multiwavelength experiments, this uniformity is not highly crucial.

As of this writing, there has not yet been an opportunity to compare the optical and thermal C_n^2 with the three-wavelength variances of log amplitude scintillation. However, on one occasion the thermal C_n^2 was measured simultaneously with the one-mile scintillations at 4880 Å on a low-turbulence day, resulting in a probably-fortuitous agreement of 7% of the theoretical variance.

To summarize, development is complete on these instruments, which will now be utilized as follows:

1. All simultaneous multiwavelength measurements of log-amplitude variance, covariance, probability distribution, and amplitude scintillation will be backed up by concurrent thermal and short-range optical determinations of C_n^2.

2. Experiments relative to the atmospheric model per se will be conducted to

a. Investigate any non-gaussian or spiking behavior in the temperature fluctuations.

b. Investigate the validity of the "2/3 law" throughout the inertial subrange through variable probe-separations.

c. Investigate the extent of the inertial subrange. using "b" for the outer scale (and possibly large inner scale conditions) and spectral cut-off of the inner scale.

d. Investigate the validity of the theoretical 5/3 (or rms 5/6) spectral characteristic of thermal fluctuations.

e. Investigate path length and height dependence of C_n^2

The validity and extent of the subrange is especially of interest during inverted and low-wind conditions, as discussed in Section III.

III. DISCUSSION OF THE CURRENT STATE OF THE TURBULENCE SCATTERING PROBLEM

As a result of discussions, meeting, and preliminary experimental results, it has become apparent that a critical review of recent experiments

and theoretical efforts is desirable in order to put the overall problem in perspective and to guide the experiments which are now commencing.

In discussing those aspects of scintillation which are not understood, we must address ourselves to (1) the range of validity of the atmospheric model, (2) the mysterious problem of the parametric dependence of saturation or multiple scattering, and (3) the influence of transmitter apertures. We will first review the results of other experimental efforts, and then consider the theoretical status.

A. EXPERIMENTS

The saturation of scintillations has been observed in Russia,[15,16] and by Deitz,[17,18] Lawrence and co-workers,[8,19] and Fried[10]. It is important to review just what was measured, and how well the results present a consistent picture.

As discussed in Appendix B, there are several second-order moments which have been used by experimentalists and theoreticians. Some of the inter-relationships (Appendix B) are dependent on an assumption of log normality of the scintillations. Furthermore, ambiguities and actual errors in these interrelationships have appeared in the literature. A consistent notation and definitions are given in the Appendix and summarized here:

$C_\ell(0)$ ≡ log amplitude variance

$C_I(0)$ ≡ log intensity variance ≡ $4C_\ell(0)$

σ_I^2 ≡ normalized intensity variance

σ_T^2 ≡ $\log_e \langle I^2 \rangle / \langle I \rangle^2$, where I is the intensity

In the early saturation measurements, Gracheva[15,16] utilized an incoherent source in a quasi-plane-wave configuration (80 mm diameter lens with a "slightly divergent" beam) to measure σ_T^2. Then, with the assumption of log normality, the saturation of $C_I(0)$ at a value of 2.56 is inferred. DeWolf[20] has pointed out an error in the data reduction, such that the saturated $C_I(0)$ is 1/4 of this or 0.64, implying a saturated log amplitude variance $C_\ell(0) = 0.16$. In view of subsequent measurements by others, it must be concluded that this value is too low. It should be pointed out that the source was not well defined, and that the assumption of log normality is quite critical since small departures can result in an apparent saturation.[21]

Other investigators have worked with quasi-point-sources (spherical waves), as follows:

Deitz[17] utilized a sophisticated photographic technique to determine σ_I^2 and, again assuming log normality, inferred a saturated value of $C_I(0)$ which essentially agrees with that of the corrected Gracheva data. In this measurement, the transmitter had an approximately 1.7 mRad divergence and 5 cm diameter, and it was found that a divergence decrease to one mRad resulted in an increase in the saturated variance to unity. The corresponding $C_I(0)$ is 0.25. In view of the discussion of Section II, it is apparent that the larger divergence was not sufficient to ensure point-source behavior, due to the 5 cm aperture; and, in fact, the general conclusion of Figure 1, i.e. that divergent, large apertures lead to greater variances than point sources, is supported in Deitz's non-saturated data. It should be noted that the influence of the log-normality assumption was again a factor.[21]

In more recent measurements[18], Deitz and Alcaraz utilized a 5 cm transmitter with a 1.9 milliradian divergence to obtain saturation at $C_\ell(0) = 0.25$ with a fall-off to 0.16. In this work, the log normality assumption was removed, since both $C_I(0)$ and σ_I^2 were measured.

Lawrence utilized a 5 cm transmitter with a 1 milliradian divergence to directly obtain a saturated $C_\ell(0)$ of 0.7. Again, the variances in the non-saturated region were larger than predicted by theory, as in Figure 1, and the transmitter may have failed to represent a point source.

In the recent Emerson Dry Lake experiments,[10] transmitter apertures of 2-5 mm were employed. At 3 mm, the inverse Fresnal number is approximately 25, so that these measurements may have represented a better approximation to a point source determination. $C_\ell(0)$ was again directly measured to saturate at a maximum of 0.7. The theoretical predictions were "corrected"[5] for the finite aperture, but in the wrong direction (predicted variances less than for a point source). This is again a manifestation of the phenomenon of Figure 1: deliberate divergence results in greater scintillation.

It is seen that there is a significant range in the "saturated" variances reported to date. The higher value of 0.7 for $C_\ell(0)$ is substantiated by measurements made earlier on this program with a finite aperture. However, we are only now beginning experiments with a true point source transmitter, which should resolve the question. The sample measurements in Table II indicate a variance at visible wavelengths which is definitely in excess of the Deitz and Russian values; furthermore since independent C_n^2 determinations were not included, it is impossible to say whether or not this variance yet represents saturation.

The importance of determining the variances and parameter breakpoint for saturation, free of transmitter aperture influences, is now clear. It may be noted that log amplitude variances of 0.25 and 0.7 represent greatly different scintillation-dynamic-ranges, which is of considerable practical importance.

B. THEORETICAL ASPECTS

The well known single-scattering (Rytov) prediction for log-amplitude variance of a spherical wave is[6]

$$C_\ell(0) = 0.124\ C_n^2\ k^{7/6}\ L^{11/6} \qquad (1)$$

where k is the optical wavenumber and L is the distance (range). The plane wave prediction is 2.5 times larger.[11] Also, within this Rytov realm, solutions for transmitter aperture effects have been obtained.[2-4] Theoretical efforts are currently concentrated on predicting at least the parameter breakpoint and general character of saturation (multiple scattering),[20,22,23,24] but it is not clear that definitive progress has been made, as discussed below. The important question of the consistency and range of validity of the atmospheric model is also under active consideration,[4,17,18,25] and will also be discussed in this section.

1. Saturation

Theoretical predictions of saturation involve the breakdown of the Rytov approximation, which for many purposes seems no more useful than the first-Born approximation. There are inherent inconsistencies in the Rytov approximation outside the first-Born region. In addition, there is some confusion in the literature over the nonzero value of the mean log amplitude and the distinction between variances and second (noncentral) moments. This will be discussed in a later report.

Theoretical investigators have been generally concerned with expressing an actual or true $C_\ell(0)$ vs. the Rytov-predicted value of Eq. (1), as the turbulence (C_n^2) and path length (L) increase.[26] In such an effort, DeWolf[20] predicted an asymptotic saturated value for $C_I(0)$ of ln 2 as the Rytov-predicted value approaches infinity. This is consistent with the corrected Russian data.[15,16] However, as pointed out above, it is significantly less than experimental values.* The analysis furthermore

*It should be noted that experimental results for $C_{\ell,I}(0)$ vs. $C_{\ell,I_{Rytov}}(0)$ (increasing C_n^2 or path length) show a maximum and small negative slope as the Rytov-predicted value continues to increase, so that the asymptote may be smaller than the values observed under moderately saturated conditions.

predicted Rayleigh, rather than log normal, statistics for strong scintillations. Like the Russian experiments, DeWolf's analysis was in terms of σ_I^2 or σ_T^2, whose relationship to $C_{I,\ell}(0)$ (as measured in the U.S.) depends rather sensitively on the log normality of the statistics.[21]

In more recent work,[22] DeWolf has acknowledged the log normal -- rather than Rayleigh -- nature of various experimental results. It was surmised that high-irradiance fluctuations are sufficiently separated in time that each involves a different instantaneous path, which leads to log normal rather than Rayleigh statistics. He then assumes that the departure from Rayleigh statistics in his saturation calculation occurs far enough out on the tail of the distribution to leave that calculation valid. However, in a final footnote he acknowledges that values of $C_I(0)$ measured in the U.S. have been higher than ln 2, so that even this assumption is questionable. It is therefore apparent that much more work is required here.

In another recent theoretical effort,[23] the renormalization technique and ordering arguments have been applied to obtain a saturation result similar to but somewhat more detailed than DeWolf's. Although the validity is unestablished, the analysis has very interesting aspects. Unfortunately, this analysis to date has employed a gaussian rather than Kolmogorov atmospheric model, which leads to parameter dependencies which may differ seriously from those of the "correct" model. For instance, the log amplitude variance in the Rytov realm depends on $(\overline{\Delta n})^2\ \ell\ Lk^2$, where n is the refractive index and ℓ is a turbulence scale factor. This is sufficiently different from the $C_n^2 k^{7/6} L^{11/6}$ prediction of Eq. (1) to render any resultant parametric conclusions doubtful. The analysis is again in terms of σ_T^2, which relates to the measured $C_{\ell,I}(0)$ only for log normal statistics.

One result is that the predicted limit as $\overline{(\Delta n^2)}$ goes to infinity is

$$\lim \sigma_T^2 = \ln\left[2 + \frac{4m^2}{4m^2 + 1}\right] \qquad (2)$$

where $m = \frac{k\ell^2}{4L}$. This asymptote, which may be identified with $C_I(0) = 4\,C_\ell(0)$ for log normal statistics, ranges between ln 3 and ln 2, the higher value representing short wavelengths and/or path lengths. For visible wavelengths, the predicted value is still low, and the wavelength-dependence (e.g. at 10 microns) is obviously quite weak, which may or may not agree with our future experiments. The limit for constant C_n^2 and increasing L is ln 2, as in Refs. 20, 22.

It is interesting to note that the complete curves[23] for $\sigma^2_{T\,\text{predicted}}$ vs. $C_I(0)_{\text{Rytov}}$ exhibit the maximum and fall-off reported by experimenters. The general results involve a somewhat complex function, from which a broad range of numerical curves have not yet been derived. Agreement with the Russian data[15,16] is demonstrated, although the parameter ℓ is chosen to effect this agreement. Rayleigh statistics are predicted for the limiting case.

It is to be hoped that the approach of Ref. 23 will be extended to the Kolmogorov atmosphere, so that the weak wavelength-dependency and low value of saturated σ_T^2 at visible wavelengths may be critically examined. If our experiments firmly establish a low value of variance saturation at 10.6 microns, the existing analysis will be disproven; on the other hand, if the 10.6μ point-source results for high C_n^2 continue to agree with Rytov predictions up to levels comparable to saturation in the visible, the present prediction will merit considerable attention.

2. Transmitter Aperture Dependence

Since the gross details of saturation with a point source are not yet understood, it is clear that little can be said about transmitter aperture dependence under saturated conditions before the experiments are

performed. However, as pointed out in Ref. 18, some of the details of apparent saturation curves may involve transmitter aperture effects within the single-scattering realm. Referring to the theoretical curve in Figure 1, if we start out in the near field of a collimated beam and then increase the range L, the value of N increases proportionately. Hence, the log amplitude variance will grow more slowly than $L^{11/6}$, and a resultant curve of observed vs. theoretical point-source (or plane wave) variance will exhibit some of the characteristics of saturation. The effect is not strong enough to explain the reported range-dependent saturation measurements, but can definitely affect the knee of the saturation curves in Refs. 15-17.

This phenomenon illustrates the importance of obtaining fundamental saturation data with a virtual point source. At the same time, experiments to confirm the transmitter aperture theory under single-scattering conditions are highly important.[18]

3. The Atmospheric Model

The range of validity of the inertial subrange model has yet to be firmly established. On very calm days, for instance, there seems to be insufficient energy to establish the subrange, and hence there is no applicable theory even though anomalously large and non-log-normal scintillations are observed.[10] Even under "normal" conditions, there may be a non-gaussian or spiking behavior of Δn (Ref. 10), which would negate the usual argument for a log normal (Rytov) wave function.[24] This may be related to an observed breakdown in 2/3-law behavior near the ground.[27,28]

These spikes represent refractive index spectral characteristics outside the outer scale, and necessitate probability-slope deriviations for a useful C_n^2. Furthermore, if the outer scale is sufficiently small that substantial portions of the optical filter function are weighted by

a non-Kolmogorov spectrum, then existing theory is inadequate for even single-scattering predictions. This condition is also postulated as occurring under diurnal inversion conditions, during which qualitatively different scintillation patterns have been observed and C_n measurements (low) have ceased to correlate with variance measurements (high).[17] A further confirmation of this condition was that temperature correlations increased with increasing probe separations, indicating that the separations were larger than the outer scale.[17]

Even when the inertial subrange is established and the outer scale is "typical" it is important to investigate the effects of a nonzero inner scale. The inner scale is believed to be typically 1 mm, and is assumed to be zero in many single-scattering theoretical developments. (The usually-stated condition is that the receiver must be in the far field of the inner scale.[6,11]) Carlson has shown[4] that an inner scale on the order of 1 cm or more can substantially reduce scintillations for point-source transmitters. The analysis simply involves setting the refractive index spectrum to zero for those wavenumbers which correspond to dimensions less than the inner scale. Evidence[18] suggests that the inner scale may be typically between 2.1 and 5.8 cm under neutral conditions.

It is apparent from the above considerations that the extent of the subrange itself must be carefully studied. The breakdown of the outer scale may be observed with variable probe separations. The inner scale is more difficult, since it is not possible to obtain reliable measurements with very-closely-spaced probes. The use of scintillation experiments per se to measure the inner scale has been suggested,[4] but possibly represents a circular corroboration in the present state of the relevant theories. The most fruitful approach is thought to be the measurement of the temporal spectrum of temperature fluctuations.[25]

In view of the above discussion, the importance of monitoring the subrange -- as opposed to simply determining C_n^2 -- is very clear.

C. DIMENSIONAL ASPECTS

As discussed in the preceding report, the existence of a breakpoint for saturation or multiple scattering raises serious dimensional difficulties, especially if the point-source saturated variance level is definitely proven to be wavelength-dependent. That is, if the critical condition for saturation is not simply that Eq. (1) becomes some fraction of unity regardless of wavelength, pathlength, or C_n^2, then the parameters of Eq. (1) are seemingly insufficient to explain a breakpoint from direct dimensional reasoning. Livingston has suggested[25] that the single parameter C_n^2 is insufficient to characterize the medium under the onset of multiple scattering, and it is not clear how the simple incorporation of a turbulence scale will alleviate the problem. This question of a dimensionless breakpoint is the single most paramount issue in the saturation of scintillations, and in principle rises above questions of the validity of particular theories; all that is needed is a proper definition of the relevant parameters.

It will be highly useful if a Kolmogorov atmosphere can be utilized in a substantiated derivation of an asymptotic expression such as that of Eq. (2). The result times four may then be set equal to the right side of Eq. (1) in order to define a breakpoint. For instance, a critical distance L_{cr} may be defined as a function of other parameters, and the hypothesis that the amplitude correlation length "saturates" as $(\lambda L_{cr})^{1/2}$ may be tested.

The correct statement of the dimensionless breakpoints may be somewhat more complicated than many dimensional analyses. For instance, a function which would ostensibly satisfy the requirements

might look like Eq. (3):

$$\sigma^2 = \frac{1}{A} \ln \left[1 + \frac{A \sigma_1^2}{(1 + B \sigma_1^2)} \right] , \qquad (3)$$

where σ^2 is the actual variance and σ_1^2 is the Rytov prediction. Such a function gives $\sigma^2 \approx \sigma_1^2$ at low variances, exhibits a maximum, and has an asymptote $(1/A) \ln [1 + A/B]$. The breakpoint would be given by $\sigma_1^2 = (A\text{-}B)^{-1}$, with the wavelength dependence, etc. appearing in the dimensionless constants (A,B).

IV. FUTURE PLANS

In view of the above considerations, the program plan given in the preceding report may be restated as follows. In order of priority, we will:

1. Gather comprehensive point-source multiwavelength data with optical and thermal C_n^2 backup under saturated and non-saturated conditions.

2. Investigate the extent of the inertial subrange under various conditions, as described above.

3. Investigate transmitter-aperture effects under saturated and non-saturated conditions.

4. Conduct receiver aperture-averaging experiments.

The experimental systems and techniques for all of these determinations are complete. The rate at which the data can be gathered will depend primarily on weather conditions.

In order to properly utilize the investment which has been made on this program, it is suggested that a final, additional one-year period be allotted. This will permit data-taking during the critical summer months of high turbulence, and will ensure that all of the relevant questions are pursued. If time permits, this follow-on period could include measurements over a longer path. No further instrumentation will be developed; the entire effort will be on measurements and interpretation.

APPENDIX A: Thermal Index-of-Refraction Instrumentation

The most sensitive means of measuring the fluctuating temperature difference between two fine-wire probes is to utilize an audio frequency carrier driving a balanced bridge which contains the probes as two of its elements. This technique overcomes 1/f-noise sensitivity limitations and permits the use of a very-low-noise front-end amplifier. The tendency for the bridge to continually drift out of balance suggests the use of a long-time-constant feedback-stabilization feature. This system will now be described in detail, including calibration and operating characteristics.

1. Circuit

The circuit is shown in Figure 6. Modular (Burr-Brown Corp.) elements are utilized throughout.

The bridge is driven with a 10 kHz oscillator, and its output is transformer impedance-matched to the input of a low-noise amplifier (noise figure = 2 dB). After further amplification, and filtering in a 2 kHz passive bandpass filter, the signal is fed to an amplifier which is manually gain-switched in six steps of $(10)^{1/2}$ each. Following this, the signal is demodulated in an active precision rectifier circuit and low pass filter. At this point, an output is provided which is linearly proportional to the temperature fluctuations (ΔT), for purposes of probability and spectral analysis.

The demodulated signal (ΔT) is then a.c.-coupled with a long (0.8 sec) time constant through buffers to a bipolar squaring module which current-feeds the summing point of a following operational amplifier. In the final stage, the resulting d.c. signal $<\Delta T^2>$ is averaged in an integrator which is provided with short (1.8 sec) and long (1 minute) time constants. The result appears on a 500 microamp meter and is available as a d.c. output voltage.

The bridge constitutes a "balanced modulator" with cancelled carrier, which would result in an output envelope proportional to $|\Delta T|$. To restore the carrier and hence achieve the desired linear amplitude modulation, it is possible to use gated or synchronous detection with a reference input from the oscillator. However, a small, deliberate bridge imbalance creates the same effect while providing a simple means of achieving feedback stabilization.

The output of the demodulator-filter is d.c. coupled through a slow integrator to optically-coupled variable-resistor elements which are in parallel with the bridge arms. The degree of bridge imbalance is controlled by an adjustable d.c. offset at the input to the integrator. The loop gain is maintained constant as the signal gain is varied, by means of a coupled switch as shown.

The action of the feedback circuit is much slower than the a.c. coupling time constant in the output signal path, so that slow drifts are cancelled without affecting the reading. This is permissible because the static temperature or resistance difference between the probes is not of interest.

In order to provide a small, incremental bridge imbalance free of hand effects, for calibrating purposes, a reed relay is utilized. When driven by a slow square-wave generator, this feature permits easy calibration and a gain-stability check of the system.

In order to realize the maximum possible dynamic range, the levels are chosen so that saturation (± 10 volts) occurs simultaneously in various elements. Instantaneous saturation peaks are indicated by means of a peak detection circuit and light-emitting diode.

The circuit is powered with rechargeable Ni:Cd cells. Meter switching at the output provides capability for monitoring the battery levels, carrier (bridge offset) level, and output proportional to C_n^2.

2. Operation

Operation of the system is quite simple. With the feedback loop opened up and caps on the probes, the bridge is balanced by monitoring the demodulator output and manually trimming the resistance and capacitance at the bridge. The feedback is engaged and set for a carrier level equal to half the saturation voltage, to permit a maximum linear modulation range. (This carrier condition is maintained automatically as the gain is varied.) The unit is faced into the wind with the desired height and probe separation, and the probes are uncapped. The gain is increased until occasional saturation is noted, and then backed-off one step. Each gain step, after squaring, represents a change in C_n^2 sensitivity by a factor of ten.

The system will stably monitor C_n^2 at the output meter. It is necessary to record the meter reading, gain setting, barometric pressure, and temperature. Through the use of a long coaxial cable and the scintillation computer electronics, the probability distribution and spectrum of the temperature fluctuations are readily analyzed; in the case of the spectrum, one probe may be capped so that absolute fluctuations are measured.

If the unit is taken from a warm environment into a cold weather condition, the capacitance drift may eventually require rebalancing. In any fully-automatic version of this system, such as in balloon experiments, it will be necessary to use temperature-compensated circuitry, or alternatively, quadrature synchronous detection may be employed with varactor diodes to automatically cancel capacitance imbalance.

3. Linearity Considerations

The bridge output is related to an incremental imbalance by a simple Thevenin equivalent circuit. If we let R_1 = fixed bridge arms, R_2 and $(R_2 + \Delta R)$ = the probe resistances, R_s = oscillator source resistance,

V_s = oscillator voltage, and R_L = transformer-coupled load resistance, the bridge output may be shown to be

$$V_{out} \simeq V_s \frac{R_1 \Delta R R_L}{(R_1 + R_2)(2R_s + R_1 + R_2)\left(R_L + \frac{2R_1R_2}{R_1+R_2}\right)} \qquad (A-1)$$

In this expression, it is assumed that $\Delta R/R_2 << 1$. Now, ΔR will consist of a deliberate offset or "bias", plus the a.c. temperature fluctuations. Under conditions of highest turbulence, the thermal/resistance coefficient of the platinum probe wires is such that $\Delta R/R_2$ is on the order of 10^{-2}, which also determines the maximum necessary bias. Hence, linearity is not noticeably degraded.

The effects of capacitive imbalance may be examined by replacing ΔR above by ΔZ. (Symmetrical or balanced capacitance components will also affect the bridge gain; e.g., replace R_1 by Z_1). It is found that linearity is maintained if $\omega R_2 \Delta C << \Delta R_{bias}/R_2$, where ω is the carrier radian frequency. This is only a problem for long unattended periods under lowest turbulence conditions, where ΔR_{bias} is small. Automatic capacitance trim is readily employed, as discussed above, but is not necessary under our experimental conditions.

4. Sensitivity Considerations

The system described here nearly achieves the fundamental sensitivity limits set by Johnson noise. The fundamental sensitivity of the system may be calculated by first assuming a noiseless front-end amplifier, which has an equivalent input rms noise voltage given by

$$V_n = \frac{1}{2}(4KTBR_i)^{1/2}. \qquad (A-2)$$

In this expression, T may be taken as 300°K, B is 2 kHz (carrier bandwidth), and R_i is the amplifier input resistance. This may be related to an equivalent ΔT at the probes. For simplicity (and to realize the best noise figure), we take $R_1 = R_2 = R_L \cong R$. The oscillator current is $I_s = V_s/R_s$, with $R_s >> R$ so that a current source may be assumed. If the transformer turns ratio is $N = (R_i/R_L)^{1/2}$, we have

$$V_{sig\ rms} = \frac{I_s}{8} \Delta R_{rms} N \quad . \qquad (A-3)$$

The SNR is given by

$$SNR = \frac{I_s^2}{64} (\Delta R)^2 N^2/kTB\ N^2R$$

$$= \frac{I_s^2 R}{64kTB} \left(\frac{\Delta R}{R}\right)^2 \qquad (A-4)$$

$$= \frac{P\,\alpha^2 (\Delta T)^2}{16\ kTB} \qquad (A-5)$$

where α is the temperature coefficient of the probe wire ($\Delta R/\Delta T$), and P is the probe heating power ($I_s^2/4R$). The minimum or critical temperature sensitivity is thus

$$\Delta T_{cr} = \frac{4\ (kTB)^{1/2}}{\alpha\ P^{1/2}} \quad . \qquad (A-6)$$

The value of P is limited by permissible probe heating, since sensitivity to wind speed is undesirable. For the present case, $I_s = 2.4 \times 10^{-4}$, $P \approx 10^{-6}$, $\alpha = 3 \times 10^{-3}$, and hence $\Delta T_{cr} = 3.2 \times 10^{-3}$ °C. This figure must be increased according to the noise figure of the amplifier, which in our case is 2 dB. This is confirmed by direct measurment.

The above appraisal is overly conservative when it is realized that noise, within the 2 kHz bandwidth, merely contributes an offset in the squared, averaged output. The constancy of this offset is what really counts, and hence the effective noise bandwidth is on the order of the reciprocal of the integration time, or 4-5 orders of magnitude less than the 2 kHz value used above. For example, with the present unit set at its highest gain, with which one may readily measure turbulence levels lower than ever realized at the ground (see below), the noise-offset is still not discernible on the meter.

The choice of probe wire diameter is an important design factor. This choice is a trade-off between fast response on one hand, and ruggedness and higher sensitivity on the other. The higher sensitivity with larger wires is due to the larger probe heating power P which is permitted as the surface area increases. The response to fast ΔT components can be increased electronically, but noise is also enhanced. In the present system, chopped-laser measurements showed adequate thermal response with probes of 2-micron diameter, where P is on the order of 1 microwatt.

5. Calibration and Measurement Range

The meter output is related to the square of the fractional bridge imbalance, as follows:

$$V_{out} = K \frac{(\Delta R)^2}{R^2} , \qquad (A-7)$$

which defines K. The temperature structure constant [11] is

$$C_T^2 = \frac{\langle \Delta T^2 \rangle}{r^{2/3}} = \frac{(\Delta R/\alpha R)^2}{r^{2/3}}$$

$$= \frac{V_{out}}{r^{2/3} K \alpha^2} , \qquad (A-8)$$

where r is the probe separation. In this expression, the factor K is determined through the use of the calibrating ΔR built into the instrument, as described above. The final necessary expression relates C_n^2 to C_T^2 (Refs. 12-14):

$$C_n = \frac{77.6\ P}{T^2} (1 + 0.00753/\lambda^2)\ 10^{-6}\ C_T, \qquad \text{(A-9)}$$

where P is barometric pressure in millibars, λ is in microns, and T is in °K. For operating convenience, this is reduced to an expression at each wavelength in terms of the pressure in inches and the temperature in °F.

The parameter K is a function of the gain setting. The useable range of the instrument covers values of C_n^2 from $1.24 \times 10^{-11}\ m^{-2/3}$ to $1.24 \times 10^{-17}\ m^{-2/3}$, which more than brackets values ever observed at the ground.

6. Spectral and Probability Analysis

As with the scintillations, the spectrum of the ΔT signal is analyzed with a Tektronix Type 1L5 unit. Since this instrument is linear in amplitude, a falloff exponent of -5/6 vs. frequency is expected according to the one-dimensional Kolmogorov result. To examine this in detail, it is possible to use the analyzer in a logarithmic mode, so that the slope of a log-log plot may be precisely determined.

The probability distribution of ΔT is analyzed in the scintillation computer. ΔT is related to the linear output voltage through gain calibration, and the variance $\langle \Delta T^2 \rangle$ is determined from the slope on gaussian probability paper. C_n^2 is then determined from (A-8) and (A-9). The presence of nonlinear "tails" on the probability plot indicates components outside the inertial subrange, as discussed in Section III.

APPENDIX B: Notation, Definitions, and Relationships for Scintillation Quantities

1. Basic Quantities

u = complex optical wave amplitude (rms)

$u_o = \langle |u| \rangle$

$\ell = \ln (|u| / u_o)$ = log amplitude (normalized)

$\psi_1 = \ln (u/u_o)$ = Rytov wave function

$\ell = \mathrm{Re}\,(\psi_1)$

I = intensity $= |u|^2$

$I_o = u_o^2$

$\ell = 1/2 \ln I/I_o$

Important identity: $\ell - \langle \ell \rangle = \ln|u| - \ln u_o - \langle \ln|u| \rangle + \langle \ln u_o \rangle$

$= \ln|u| - \langle \ln|u| \rangle$

Hence, the log amplitude is obtained electronically by a.c. - coupling the logarithmic signal.

2. Moments:

$C_\ell(0) = \langle (\ell - \langle \ell \rangle)^2 \rangle$ = log amplitude variance

$C_I(0) = \langle (\ln I - \langle \ln I \rangle)^2 \rangle$ = log intensity variance

$$\sigma_I^2 = \frac{(I - \langle I \rangle)^2}{\langle I \rangle^2} = \text{normalized intensity variance}$$

$$\sigma_T^2 = \ln \frac{\langle I^2 \rangle}{\langle I \rangle^2}$$

3. **Relationships:**

$$C_I(0) = 4\, C_\ell(0)$$

$$\sigma_T^2 = \ln (1 + \sigma_I^2)$$

If the statistics are log normal, then

$$\sigma_I^2 = e^{C_I(0)} - 1$$

$$C_I(0) = \sigma_T^2$$

REFERENCES

1. F.P. Carlson, E.E. Department, University of Washington, Seattle, Washington, private communication.

2. Akira Ishimaru, "Fluctuations of a Beam Wave Propagating through a Locally Homogeneous Medium," Radio Science, vol.4, p.295-305, April 1969.

3. A. Ishimaru, "Fluctuations of a Focused Beam Wave for Atmospheric Turbulence Probing, "Proc. IEEE, vol. 57, p.407-414, April 1969.

4. F.P. Carlson, "Applications of Optical Scintillation Measurements to Turbulence Diagnostics," to be published in JOSA.

5. D.L. Fried and J.B. Seidman, "Laser-Beam Scintillation in the Atmosphere," JOSA, vol.57, pp.181-185, February 1967.

6. D.L. Fried, "Propagation of a Spherical Wave in a Turbulent Medium," JOSA, Vol. 57, p.175-180, February 1967.

7. These chopping wheels were developed by Carl T. Miller, Engineer on the project.

8. Robert S. Lawrence, "Experimental Results in Optical Waves," Lecture in CU/ESSA Electromagnetic Propagation Course, VII-2, 1968.

9. H. Kogelnik and T. Li, "Laser Beams and Resonators," Proc. IEEE, vol. 54, pp. 1312, 1328, October, 1966.

10. "Optical Propagation Measurements at Emerson Lake - 1968," Final Report, Contract NAS 1-7705, Autonetics, December 1968.

11. V.I. Tatarski, Wave Propagation in a Turbulent Medium (McGraw-Hill Book Co., Inc., New York, 1960).

12. "Measurement of the Refractive Index Structure Coefficient, C_n," Aberdeen Proving Grounds, BRL Rept. No. 1885, December 1967.

13. G.R. Ochs, "A Resistance Thermometer for Measurement of Air Temperature Fluctuations," ESSA Rept. No. IER 47-ITSA 46, October 1967.

References (Cont'd)

14. L.R. Zwang, "Measurements of Temperature Pulse Frequency Spectra in the Surface Layer of the Atmosphere," Izv. Geophysical Service, p. 1252-1262, 1960.

15. M.E. Gracheva and A.S. Gurvich, "Strong Fluctuations in the Intensity of Light Propagated through the Atmosphere Close to the Earth," Izv. VUZ, Radiofizika, vol. 8, p.717-724, 1965.

16. M.E. Gracheva, "Research Into the Statistical Properties of the Strong Fluctuations of Light When Propagated in the Lower Layer of the Atmosphere," Izv. Vuz. Radiofiz., vol.10, pp.775-787, 1967.

17. P.H. Deitz and N.J. Wright, "Saturation of Scintillation Magnitude in Near-Earth Optical Propagation," JOSA, vol. 59, p.527-535, May 1969.

18. P.M. Livingston, P.H. Deitz, and E.C. Alcaraz, "Coherent Light Propagation through a Turbulent Atmosphere: Measurements of the Optical Filter Function," to be published in JOSA.

19. G.R. Ochs and R.S. Lawrence, "Saturation of Laser-Beam Scintillation Under Conditions of Strong Atmospheric Turbulence," JOSA, vol. 59, pp. 226-7, February 1969.

20. D.A. DeWolf, "Saturation of Irradiance Fluctuations due to Turbulent Atmosphere," JOSA, vol. 58, pp.461-466, April 1968.

21. M.W. Fitzmaurice and J.L. Bufton, "Measurement of Log-Amplitude Variance," JOSA, vol. 59, pp. 462-463, April 1969.

22. D.A. DeWolf, "Are Strong Irradiance Fluctuations Log Normal or Rayleigh Distributed?", JOSA, vol. 59, pp. 1455-1460, November 1969.

23. M.I. Sancer and A.D. Varvatsis, "Calculation of the Maximum Associated with the Saturation Phenomenon of Light Propagation in the Atmosphere," paper TuD11, 1969 Annual OSA Meeting, Chicago, Illinois.

24. J.W. Strohbehn, "Line-of-Sight Wave Propagation through the Turbulent Atmosphere," Proc. IEEE, vol.56, p.1301-1318, August 1968.

25. Peter M. Livingston, Catholic University, Washington, D.C. , private communication.

References (Cont'd)

26. V.I. Tatarskii, "On Strong Fluctuations of Light Wave Parameters in a Turbulent Medium," Soviet Physics JETP, vol. 22, p.1083-1088, 1966.

27. Robert S. Lawrence, ESSA, Boulder, Colorado, private communication.

28. C.E. Coulman and D.N.B. Hall, "Optical Effects of Thermal Structure in the Lower Atmosphere," Applied Optics, vol. 6, pp. 497-503, March 1967.

LIST OF FIGURES

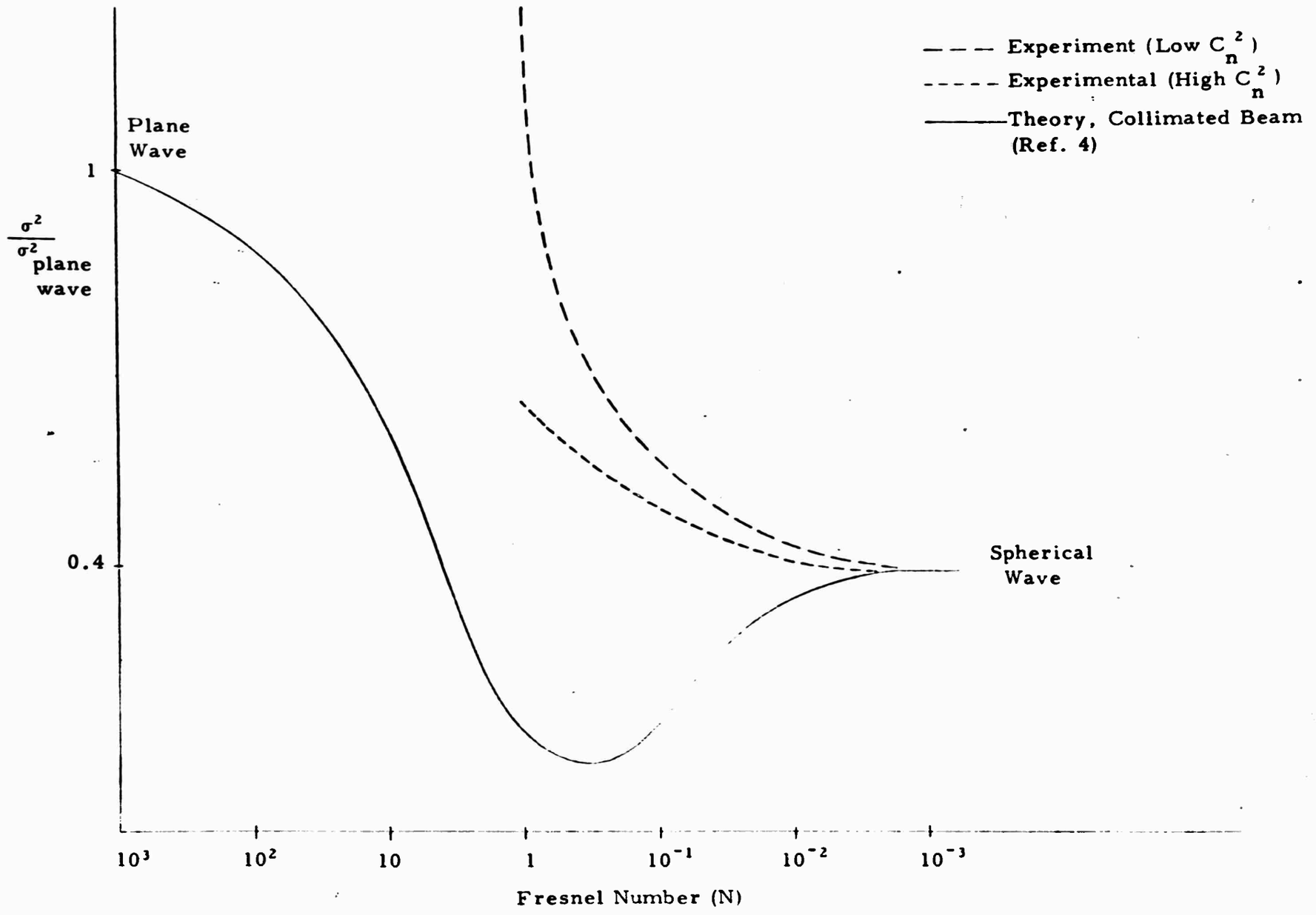
Experiment (Low C_n^2)
Experimental (High C_n^2)
Theory, Collimated Beam (Ref. 4)
Plane Wave
1
$\frac{\sigma^2}{\sigma^2_{\text{plane wave}}}$
0.4
Spherical Wave
10^3
10^2
10
1
10^{-1}
10^{-2}
10^{-3}
Fresnel Number (N)

Figure 1.

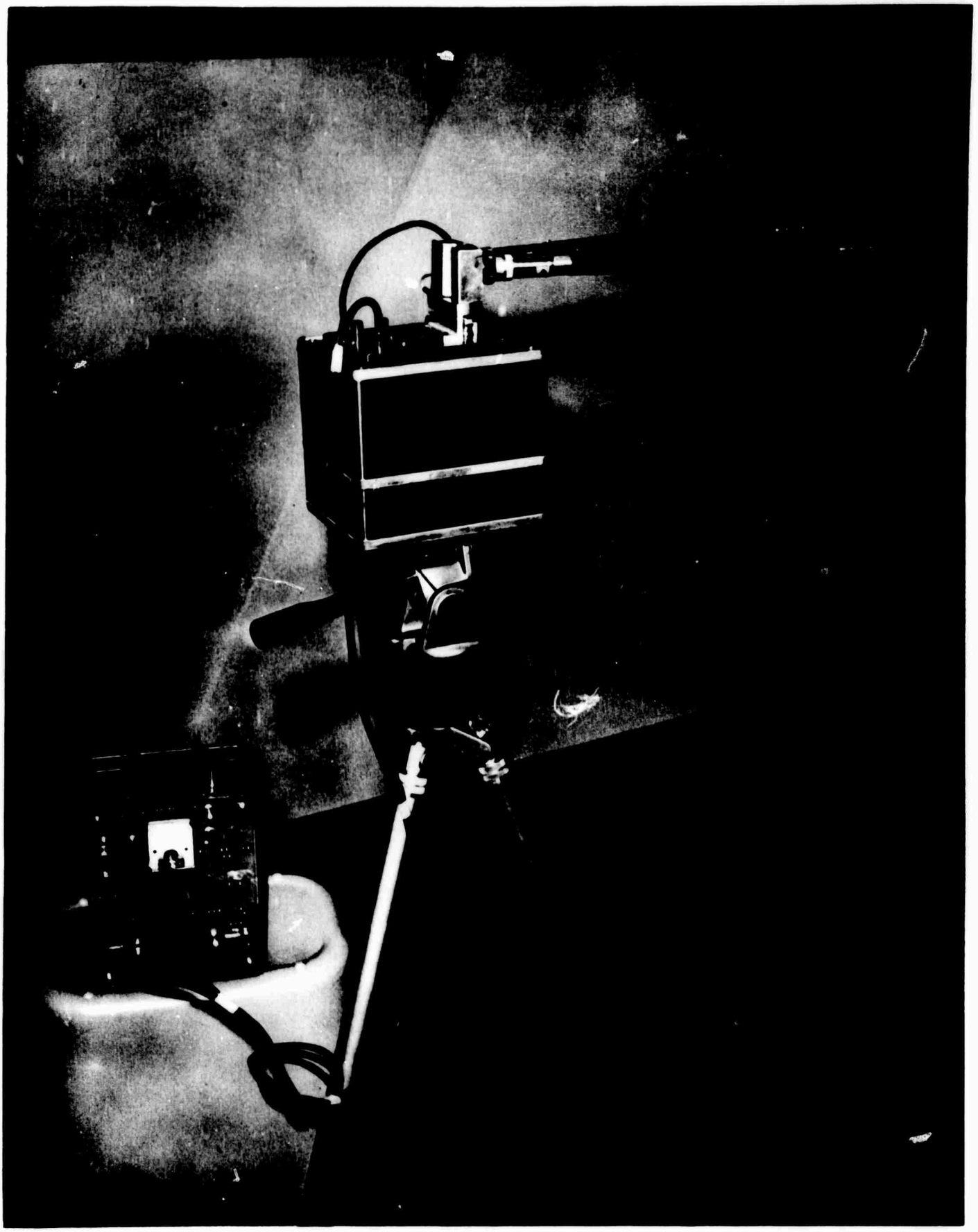

FIGURE 2

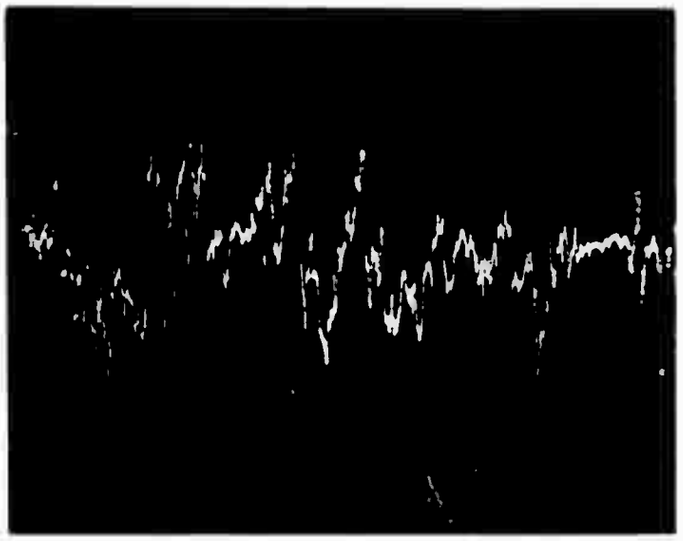

FIGURE 3

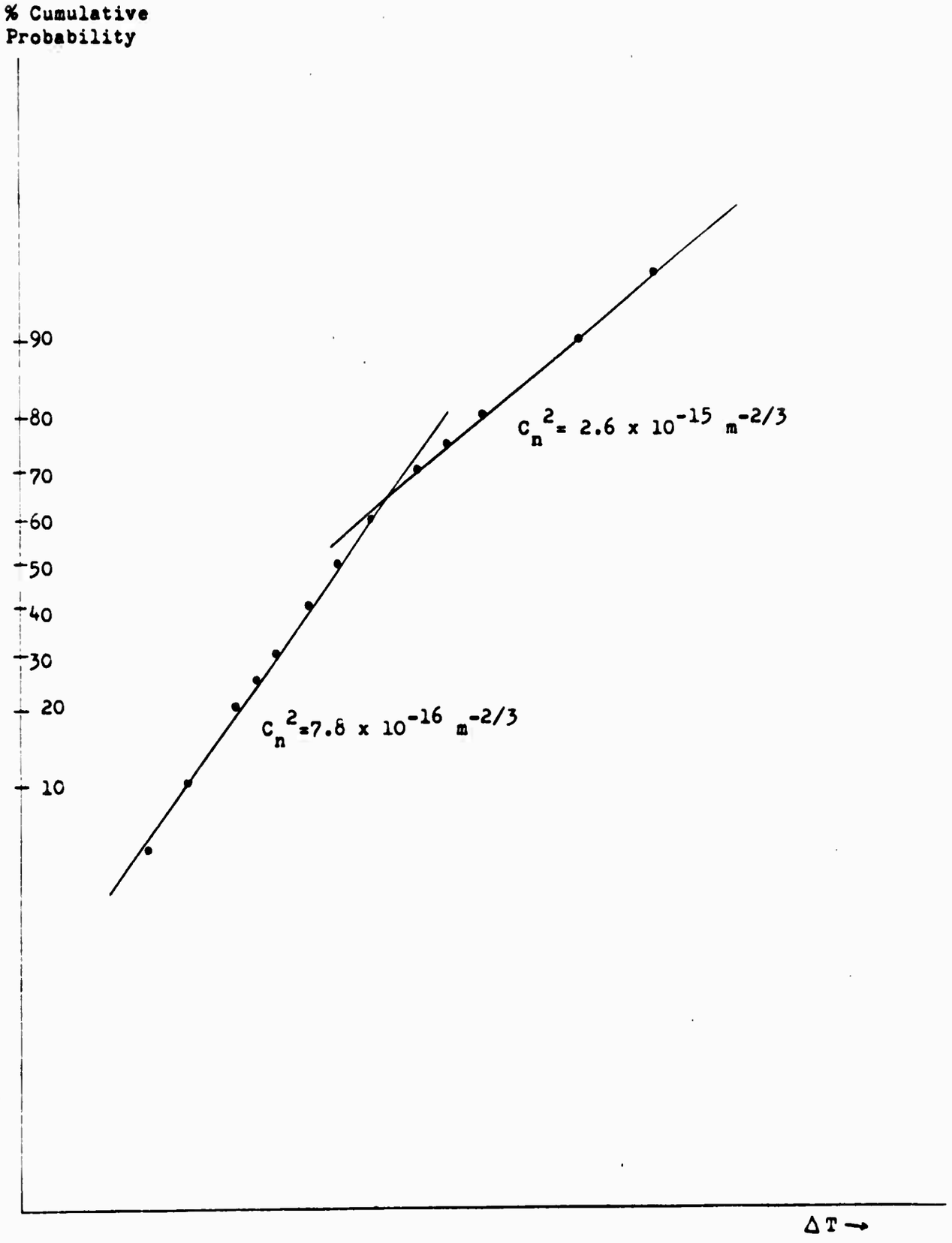
% Cumulative Probability
90
80
70
60
50
40
30
20
10
$C_n^2 = 2.6 \times 10^{-15}\ m^{-2/3}$
$C_n^2 = 7.8 \times 10^{-16}\ m^{-2/3}$
ΔT →

Figure 4

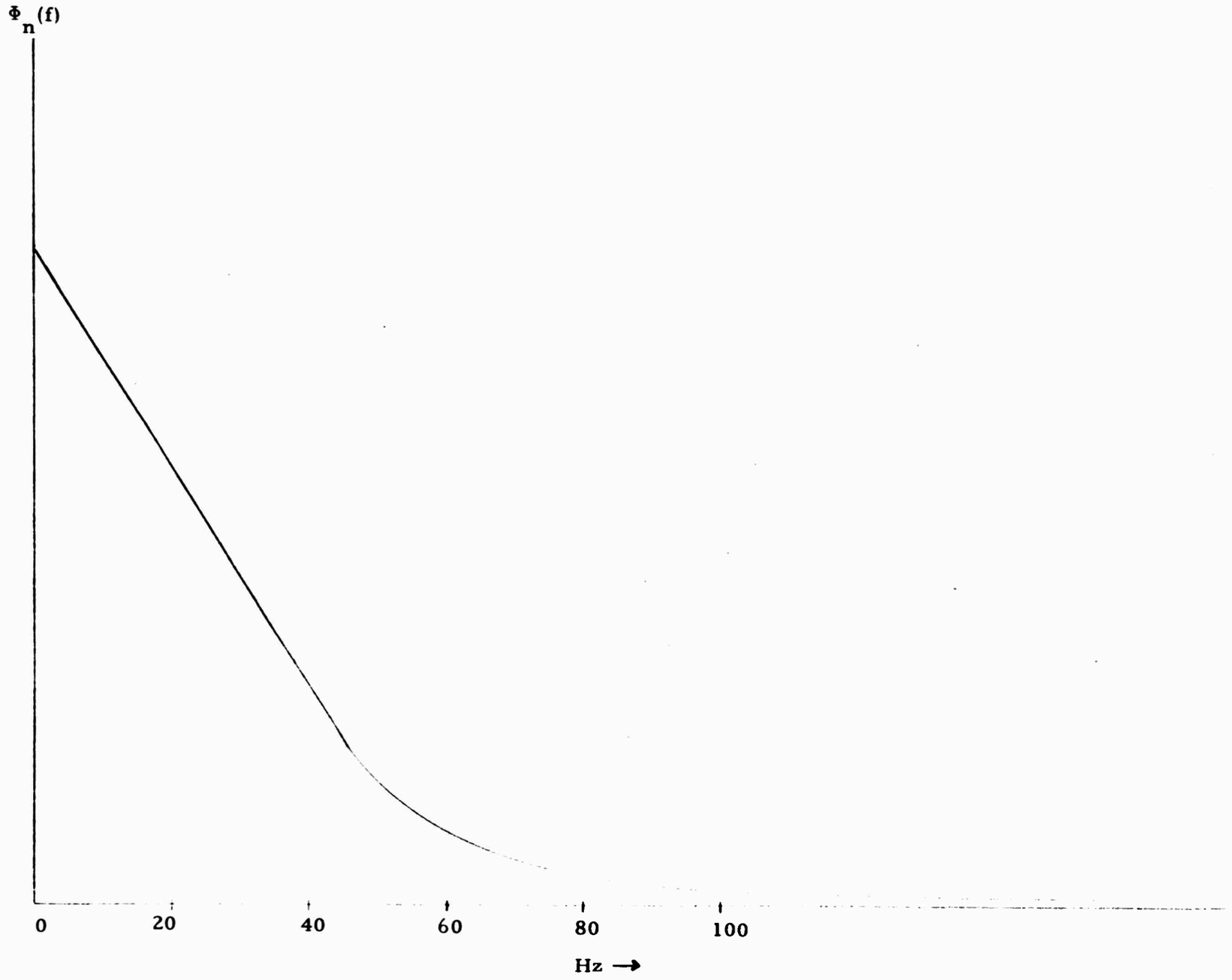

Figure 5.

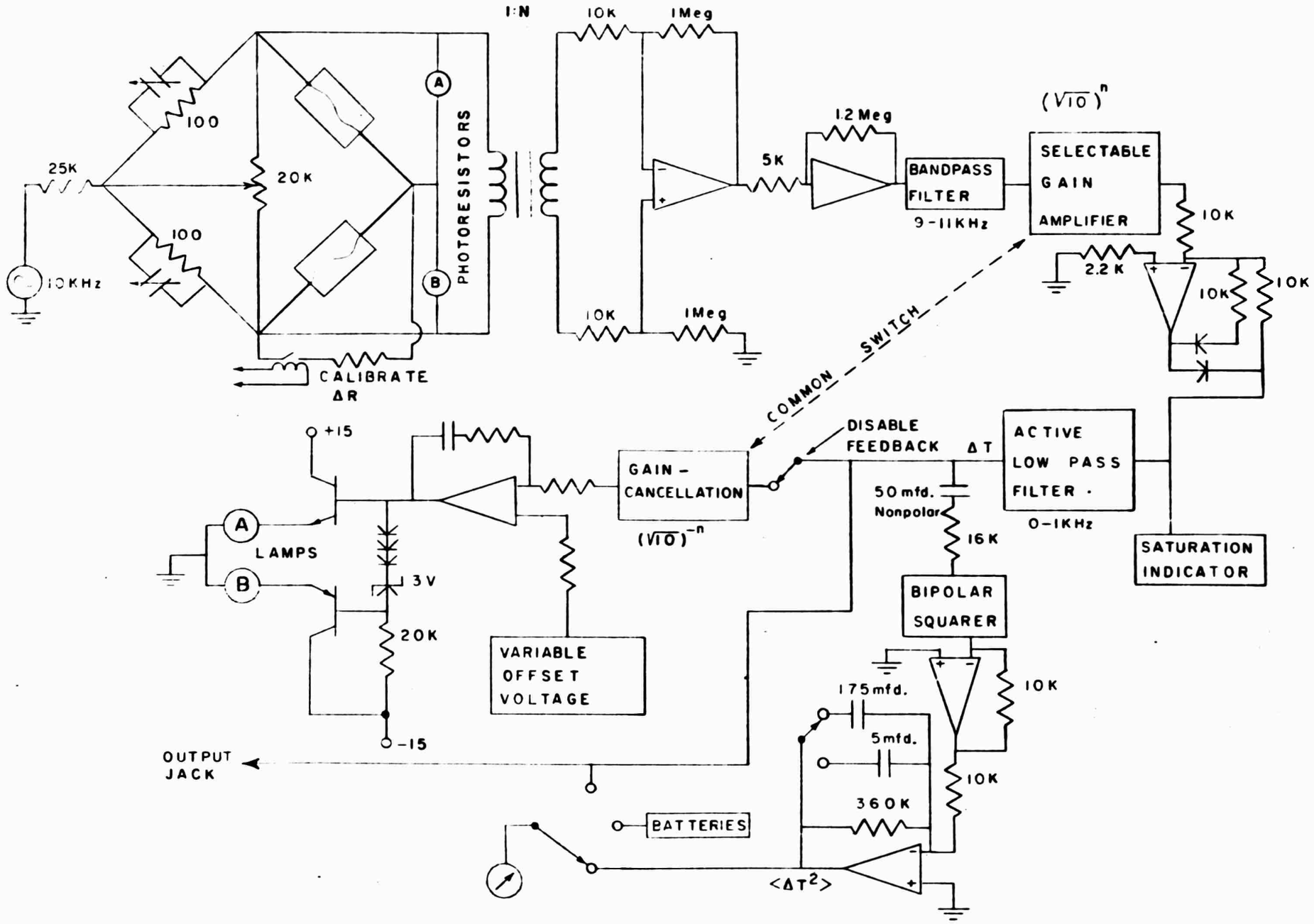
1:N
10K
1Meg
100
25K
20K
100
10KHz
A
B
PHOTORESISTORS
CALIBRATE
ΔR
10K
1Meg
1.2Meg
5K
BANDPASS
FILTER
9-11KHz
(√10)^n
SELECTABLE
GAIN
AMPLIFIER
10K
2.2K
10K
10K
COMMON SWITCH
+15
A
LAMPS
B
3V
20K
-15
GAIN -
CANCELLATION
(√10)^-n
DISABLE
FEEDBACK
ΔT
50 mfd.
Nonpolar
16K
ACTIVE
LOW PASS
FILTER
0-1KHz
SATURATION
INDICATOR
BIPOLAR
SQUARER
VARIABLE
OFFSET
VOLTAGE
175mfd.
5mfd.
360K
10K
10K
OUTPUT
JACK
BATTERIES
<ΔT²>

Figure 6

Unclassified

Security Classification

DOCUMENT CONTROL DATA - R & D

Security classification of title, body of abstract and indexing annotation must be entered when the overall report is classified)

1. ORIGINATING ACTIVITY (Corporate author) Oregon Graduate Center 9340 SW Barnes Rd. Portland, Oregon 97225	2a. REPORT SECURITY CLASSIFICATION Unclassified 2b. GROUP

3. REPORT TITLE

MULTIWAVELENGTH LASER PROPAGATION STUDY--II

4. DESCRIPTIVE NOTES (Type of report and, inclusive dates)

Quarterly; September 15, 1969-December 15, 1969

5. AUTHOR(S) (First name, middle initial, last name)

J. Richard Kerr

6. REPORT DATE January 1970	7a. TOTAL NO. OF PAGES 40	7b. NO. OF REFS 28
8a. CONTRACT OR GRANT NO. N00014-68-A-0461-0001 b. PROJECT NO. c. d.	9a. ORIGINATOR'S REPORT NUMBER(S) 1154-6 9b. OTHER REPORT NO(S) (Any other numbers that may be assigned this report)	

10. DISTRIBUTION STATEMENT

Distribution of this document is unlimited.

11. SUPPLEMENTARY NOTES	12. SPONSORING MILITARY ACTIVITY Advanced Research Projects Agency Department of Defense--Pentagon Washington, D.C. 20301

13. ABSTRACT

In conducting multiwavelength scintillation experiments over a one mile path, it was found that a finite-sized transmitter aperture does not represent a true spherical-wave source, regardless of the beam divergence used. This observation has important implications for the interpretation of other data on the "saturation" of scintillations, and in the present experiments has lead to the redesign of the transmitter to achieve a virtual point source. This has been completed, including a provision for independently increasing the aperture at each wavelength up to two inches in diameter, for later transmitter-aperture-dependence measurements.

A highly-developed thermal probe system for the detailed study of turbulence structure was made completely operational, and a portable laser system was fabricated for independent "optical turbulence strength" measurements. All subsystems of the experimental facility are operating without problems, and no further modifications are contemplated.

In order to put the problem of atmospheric scintillations in current perspective and to guide the comprehensive experiments, a discussion of recent experimental and theoretical issues is given. It is felt that the understanding of the turbulence scattering problem has progressed to the point where the correct questions may be posed and definitively investigated through these experiments.

14 KEY WORDS	LINK A		LINK B		LINK C	
	ROLE	WT	ROLE	WT	ROLE	WT
Visible atmospheric transmission						
Infrared atmospheric transmission						
Turbulence scattering						
Atmospheric propagation						